

Modeling x-ray photoionized plasmas produced at the Sandia Z-facility

P.A.M. van Hoof^{1*}, M.E. Foord², R.F. Heeter², J.E. Bailey³, H.-K. Chung², M.E. Cuneo³, W.H. Goldstein², V. Jonuskas¹, F.P. Keenan¹, R. Kisielius¹, D.A. Liedahl², C. Ramsbottom¹, S.J. Rose⁴, P.T. Springer² and R.S. Thoe²

¹ *APS Division, Physics Dept., Queen's University, Belfast BT7 INN, Northern Ireland*

² *Univ. of California, Lawrence Livermore National Laboratory, Livermore, CA 94551, USA*

³ *Sandia National Laboratory, Albuquerque, NM, 37185, USA*

⁴ *Dept. of Physics, Clarendon Laboratory, Parks Road, Oxford OX1 3PU, United Kingdom*

Abstract. In experiments at the high-power Z-facility at Sandia National Laboratory in Albuquerque, New Mexico, we have been able to produce a low density photoionized laboratory plasma of Fe mixed with NaF. The conditions in the experiment allow a meaningful comparison with x-ray emission from astrophysical sources. The charge state distributions of Fe, Na and F are determined in this plasma using high resolution x-ray spectroscopy. Independent measurements of the density and radiation flux indicate unprecedented values for the ionization parameter $\xi = 20 - 25 \text{ erg cm s}^{-1}$ under nearly steady-state conditions. First comparisons of the measured charge state distributions with x-ray photoionization models show reasonable agreement, although many questions remain.

1. Introduction

With the recent launch of the x-ray observatories *Chandra* and *XMM-Newton*, high resolution spectra from numerous photoionized x-ray sources such as x-ray binaries and active galactic nuclei are being obtained. With these instruments we are able for the first time to resolve individual lines in these spectra, and they often contain prominent lines from iron which can be used as diagnostics for the physical conditions in the plasma. However, the analysis of these lines is hampered, amongst other things, by a lack of high quality atomic data and uncertainties in the treatment of the energy balance in optically thick plasmas. As a consequence, we do not know how accurate the results from our modeling codes are. To address this problem, we have set up an experiment to create a near steady-state laboratory x-ray photoionized plasma with observationally constrained physical conditions that are astrophysically relevant. We have produced a low-density plasma of Fe mixed with NaF, and observed absorption and emission spectra of this plasma which will be used to benchmark existing astrophysical and laboratory modeling codes. These experiments are being combined with an effort to calculate high quality atomic data of relevant iron ions. In Sect. 2 we briefly describe the experiment

* email: p.van-hoof@qub.ac.uk



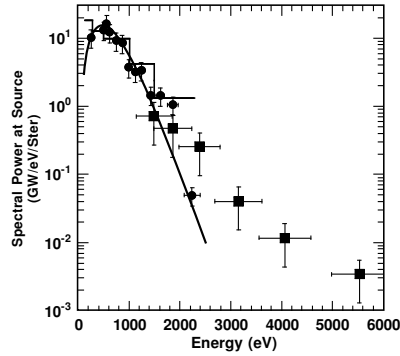


Figure 1. Z-pinch x-ray spectral emission measured at peak power with an XRD array (histogram), a transmission grating spectrometer (dots), and a PCD array (squares). The peak-normalized 165 eV blackbody fit is also shown.

and the determination of the physical parameters, while in Sect. 3 we describe the current status of our modeling effort. Finally, in Sect. 4 we briefly outline the current status of our atomic data calculations.

2. The experiment

In experiments at the high-power Z-facility at Sandia National Laboratory in Albuquerque, New Mexico, we have been aiming to produce a low density photoionized laboratory plasma of Fe mixed with NaF. The radiation from the z-pinch is generated by inductively coupling a 20 MA, 100 ns rise time current pulse into a 2 cm diameter wire array, consisting of 300 tightly strung $11.5 \mu\text{m}$ tungsten wires. The electromagnetic forces drive the wires radially inward onto the central axis, creating a 8 ns FWHM, 120 TW peak power, 165 eV near-blackbody radiation source. The emission from the z-pinch was directly observed by several spectrometers, which allowed us to determine the time-resolved history of the absolute spectral flux of the pinch. The spectrum at peak emission is shown in Fig. 1.

Free standing thin ($500 - 750 \text{ \AA}$) rectangular foils were suspended in frames and positioned parallel to the z-axis of the pinch at a distance of 1.5 – 1.6 cm. The foils consisted of a 1.35 : 1 molar ratio of Fe/NaF and were overcoated on each side with 1000 \AA of lexan ($\text{C}_{16}\text{H}_{14}\text{O}_3$)_n to help maintain uniform conditions during heating and expansion. The radiation generated during the 100 ns run-in phase preheats and expands the foil to about 1.5 – 2 mm. When the wires collide on axis, the resulting x-ray pulse quickly photoionizes the low density expanded foil. Two spectrometers were used to record the time-integrated absorption and emission spectrum of the plasma. For the absorption spectrum, the z-pinch emission was used as a backlighter. The instrumental resolution was $E/\Delta E = 500 - 800$ in the range

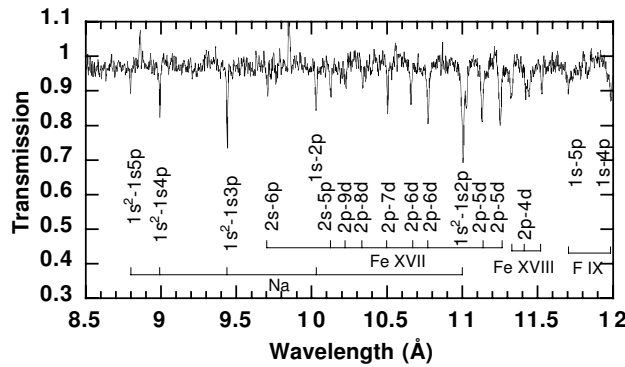


Figure 2. Time-integrated absorption spectrum of L-shell Fe and K-shell Na and F lines.

8.5 – 17 Å. A section of the absorption spectrum is shown in Fig. 2. This is weighted by the time evolution of the pinch emission, and therefore reflects conditions near the peak of the emission. To account for the estimated few ns required to reach steady-state equilibrium, the values of the absolute spectral flux and the electron density used in the calculations were taken at +3 ns after the peak of the radiation pulse, thus justifying the use of steady-state modeling codes.

The charge state distribution. To determine the relative populations of each of the charge states in the plasma, we used a curve of growth analysis which gives a relation between the equivalent width of an absorption line (this is the integrated depth of the normalized absorption line) and the abundance of a given ion. We adapted the theory to account for the expansion of the plasma in the foil. Details can be found in Foord et al., 2004, Phys. Rev. Letters (in press). The analysis was applied to the Na and F absorption spectrum shown in Fig. 2. The resulting ratio of $\text{Na}^{10+} : \text{Na}^{9+}$ ground state ions was 1 : 4.5. Similar analysis of F absorption lines indicated a ratio of 6.0 : 1 for $\text{F}^{8+} : \text{F}^{7+}$. The reversed ratio for F relative to Na is due to its lower photoionization threshold. For the Fe ions a somewhat different method was used because many of the observed lines were blended. Line positions and oscillator strengths for many thousands of Fe lines were calculated using the HULLAC suite of codes (Klapisch et al., 1977, J. Opt. Soc. Am., 67, 148). The charge state distribution was then determined by varying each Fe charge state concentration to best fit the absorption line strengths. The resulting Fe charge state distribution is shown in Fig. 3.

The density determination. To determine the density of the plasma, a time-gated filtered x-ray pinhole camera was used that imaged the Fe/NaF emission region nearly edge-on. This allowed us to determine the thickness of the plasma as a function of time. Combined with the areal density of the material in the foil (supplied by the manufacturer), we could determine the

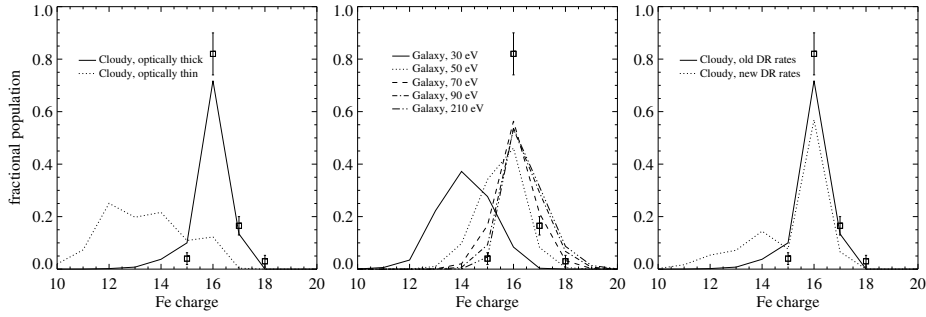


Figure 3. The experimental charge state distribution of Fe (open squares) compared to various models of the experiment.

volume density of each of the elements that were present in the plasma. The tamping effect of the lexan coating of the foil helped to maintain uniform conditions in the plasma, thus justifying this approximation. Combining this information with the charge state distribution we derived above, allowed us to determine the number density of each ionic state and finally the electron density (n_e). The resulting value is $n_e = 2.0 \pm 0.7 \times 10^{19} \text{ cm}^{-3}$ at +3 ns after the peak. When we combine the absolute flux calibration derived in the previous section with this value of the electron density, we find that we reach peak values of the ionization parameter $\xi \equiv 16\pi^2 J/n_e = 20 - 25 \text{ erg cm s}^{-1}$, where J is the mean intensity in $\text{erg cm}^{-2} \text{ s}^{-1}$ integrated from 13.6 eV to infinity. We believe these are the highest values reached in laboratory experiments to date, and are approaching the astrophysically relevant domain.

The temperature determination. We have not yet been able to identify a reliable means of obtaining the electron temperature (T_e) from the observations. Hence to obtain an estimate for the temperature, we used the astrophysical modeling code CLOUDY (Ferland et al., 1998, PASP, 110, 776). This code calculates T_e by a detailed energy accounting of all relevant heating and cooling processes in the plasma. Our first model calculation included a restricted set of Fe emission lines that effectively treated the Fe resonance lines as optically thick. This assumption is consistent with the measured saturation of the strongest Fe lines. The model yielded $T_e \approx 150 \text{ eV}$ and an average charge state $\langle Z \rangle \approx 16.0$ (see Fig. 3, left panel), in reasonable agreement with both the measured distribution width and the average ionization state. To test the sensitivity to optical depth effects, a second model was constructed which treated all lines as optically thin. This yielded a much lower temperature (38 eV), due to enhanced cooling from line emission, and a distribution that peaked at Fe^{12+} . The latter model is clearly inconsistent with the observations, but does set a lower limit for T_e . We will adopt $T_e = 150 \text{ eV}$ as our current best estimate, but we do intend to obtain independent measurements of the electron temperature in future work, e.g. through Thomson scattering.

We also aim to improve the treatment of optical depth effects in the cooling lines using escape probabilities in order to obtain better estimates of T_e from our modeling codes.

3. The modeling

The charge state distributions for Fe, Na, and F were calculated with the collisional-radiative code GALAXY (Rose, 1998, J. Phys. B, 31, 2129). For a given density, temperature, and incident radiation field, GALAXY calculates the steady-state ionization balance within the plasma. Collisional and radiative excitation and ionization, as well as autoionization and all reverse processes are included. A rate matrix is constructed that couples the initial and final levels using simple scaled-hydrogenic expressions. Accurate Hartree-Dirac-Slater photoionization cross sections are used where possible, and Kramers cross sections are used otherwise. The GALAXY code employs an average-of-configuration approximation for electronic states with a principal quantum number $n \leq 5$ and averages over all the configurations with the same principal quantum number for higher n .

To account for the estimated few ns required to reach steady-state equilibrium, the values of the absolute spectral flux and sample density ($n_e = 2.0 \pm 0.7 \times 10^{19} \text{ cm}^{-3}$) used in the calculations were taken at +3 ns after the peak of the radiation pulse. We estimate that the decrease in ξ from 25 to 20 erg cm s^{-1} during this time has a very small effect on the ionization balance. Using these values, the charge state distribution for Fe was calculated for various temperatures between 30 and 210 eV (see Fig. 3, middle panel). Above 70 eV, the distributions peak near Fe^{16+} and are quite insensitive to T_e . In this temperature regime (90 to 210 eV) calculations indicate that photoionization of Fe L-shell ions dominates over collisional ionization processes by more than a factor of ten. The weak temperature dependence of the charge state distribution therefore is likely due to the thermal electrons having insufficient energy to ionize the L-shell ions in this regime. Below 50 eV, the contribution from three-body recombination begins to dominate, reducing the degree of ionization substantially. This indicates that we succeeded in creating a photoionization dominated plasma.

The average charge state predicted by GALAXY in the 90 to 210 eV temperature range is $\langle Z \rangle \simeq 16.4 \pm 0.2$ (see Fig. 4). The uncertainty in $\langle Z \rangle$ is determined from folding in the sensitivities to the uncertainties in the absolute flux ($\pm 20\%$) and density ($\pm 35\%$) measurements. The calculated distribution is slightly more ionized than measured. This may be due, in part, to the fact that the measured time-integrated absorption spectrum is weighted by the time-history of the backlighter intensity, which peaks a few ns before the sample reaches steady-state equilibrium, resulting in a slightly lower average

charge. GALAXY calculations of H to He-like ratios for F and Na yielded ratios of 6.7 : 1 and 1 : 1.4, respectively at $T_e = 150$ eV. The F ratio agrees well with the observations, while the Na observations indicate a lower degree of ionization than the model.

Recently two papers have been published that defended the need for an update in the dielectronic recombination (DR) rates of Fe (Netzer, 2004, ApJ, 604, 551; Kraemer et al., 2004, ApJ, 604, 556), claiming that the new rates produce a better fit to *Chandra* and *XMM-Newton* data. To test this hypothesis, we made a CLOUDY model using the new rates but without any further modifications (Fig. 3, right panel). Taken at face value, this model indicates that the new DR rates give a worse fit to our observations by overpopulating the M-shell stages. We intend to investigate this discrepancy further.

4. The atomic data calculations

We are currently undertaking a comprehensive effort to calculate high quality atomic data for all the transitions that are relevant in this experiment. The current status of this effort is as follows:

Fe XIII – XIV: Kisielius et al., in preparation — we have calculated energy levels and E1 transition probabilities for L-shell photo-excitation using the Breit-Pauli approximation implemented in the CIV3 code.

Fe XV – XVI: Kisielius et al., 2003, MNRAS, 344, 696 — we have calculated energy levels and E1 transition probabilities for L-shell photo-excitation using the Breit-Pauli approximation implemented in the CIV3 code.

Fe XVII: Aggarwal et al., 2004, A&A, in press — we have calculated energy levels and transition probabilities (E1, M1, E2, M2) upto $n = 5$ using the fully relativistic GRASP code. Calculations of the collision strengths using the relativistic DARC code are in progress (Kisielius et al., in preparation).

Fe XVIII: Jonauskas et al., 2004, A&A, 416, 383 — we have calculated energy levels and transition probabilities (E1, M1, E2) using the GRASP code. Calculations of the collision strengths are in progress.

Fe XIX: Jonauskas et al., 2004, A&A, in press — we have calculated energy levels and transition probabilities (E1, M1, E2) using the GRASP code.

Acknowledgements

FPK and SJR are grateful to AWE Aldermaston for the award of William Penney Fellowships. This work was supported by EPSRC and PPARC, and also by NATO Collaborative Linkage Grant CLG.979443. We are also grateful to the Defense Science and Technology Laboratory (dstl) for support under the Joint Grants Scheme. The photoionization code CLOUDY, written by Gary J. Ferland and obtained from <http://www.nublado.org>, was used.